Response to Reviewer #4

Overview:

Comment: *The manuscript presents a timely and valuable investigation into the role of oxygenated volatile organic compounds (OVOCs) in atmospheric chemistry and regional air quality, with a specific focus on the Yangtze River Delta (YRD) region. OVOCs remain a major source of uncertainty in air quality modeling due to poorly constrained emissions, and this study addresses an important gap by incorporating updated, source-resolved OVOC emission profiles into the CMAQ model. The topic is highly relevant to both atmospheric chemistry research and practical air quality management, particularly in rapidly urbanizing and polluted regions such as the YRD. However, several aspects of the manuscript require revision before it can be deemed acceptable for publication in ACP.*

Response: We thank the reviewer for the constructive and positive feedback on our study. The comments have been very helpful in improving the clarity and overall quality of the manuscript. In response to the reviewer's suggestions, we have: (1) provided a detailed description of the methodology for constructing source profiles; (2) evaluated the impact of temporary control measures during the 2019 China International Import Expo (CIIE); and (3) made revisions to improve the accuracy and clarity of the text and figures. Detailed responses to each comment are provided below. The reviewer's comments are shown in black italics, our responses are in blue, and the corresponding revisions in the manuscript are highlighted in red.

Comments:

Comment: *1. Section 2.1: While the paper states that "source-resolved OVOC profiles derived from measurements and literature" were used, additional details on how these profiles were constructed would enhance reproducibility and allow readers to assess potential uncertainties.*

Response: Thank you for the valuable suggestion. Source profiles of the 2019YRD inventory were derived based on the 2017YRD inventory (An et al., 2021), with updates for diesel vehicles, industrial processes, biomass burning, and gasoline vehicles. Profiles of diesel vehicles, industrial processes, and biomass burning were obtained based on 160 source-resolved measurements. For diesel vehicles, twenty in-use heavy-duty vehicles from five major brands were tested, encompassing China VI (n=6), China V (n=10), and China IV (n=4) emission standards. For industrial emissions, a total of 84 samples were collected from priority sectors, including petrochemical industries, chemical raw material production, and other chemical production sectors such as plywood production, coking, pesticides production, ink production, and rubber production. For residential biomass burning, 23 samples of the combustion of four

representative biomass fuels (wood, corncob, bean straw, and corn straw) and two common coal types (anthracite and briquette coal) were collected from the stack nozzles of household stoves. For the gasoline vehicle source, the VOC (including OVOCs) profiles from published literature (Wang et al., 2022a; Huang et al., 2024) were used. A two-step process was then employed to obtain the profile of each source category:

(1) Sub-category Averaging: To minimize the influence of individual sample variability, measurements were averaged to derive stable, representative profiles for each sub-category. For example, diesel vehicle emissions were classified according to China VI, China V, and China IV emission standards, respectively. For industrial processes, representative profiles were derived according to specific industrial stages, raw materials, products, and fuel types. Similarly, for biomass burning emissions, fuel-specific profiles were established.
(2) Weighted Integration: The final integrated source profiles were synthesized by weighting the sub-category profiles according to their respective total VOC emission contributions in the study region.

We have revised the manuscript to reflect these details in Lines 116-134 as follows:
"The VOC composition of emissions from diesel vehicles, industrial processes, and residential biomass burning was characterized based on 160 localized, source-resolved measurements conducted in China. Specifically, twenty in-use heavy-duty diesel vehicles from five major brands were tested, encompassing China VI (n=6), China V (n=10), and China IV (n=4) emission standards. For industrial emissions, a total of 84 samples were collected from priority sectors, including petrochemical industries, chemical raw material production, and other chemical production sectors such as plywood production, coking, pesticides production, ink production, and rubber production. For residential biomass burning, 23 samples of the combustion of four representative biomass fuels (wood, corncob, bean straw, and corn straw) and two common coal types (anthracite and briquette coal) were collected from the stack nozzles of household stoves. Details of the sampling protocols and analytical procedures can be found in a previous study (Gao et al., 2023). VOC profiles for other sources, such as gasoline vehicles, were based on published literature (Wang et al., 2022a; Huang et al., 2024). To develop representative source profiles, a two-step aggregation method was employed. First, sub-category average profiles were derived by averaging individual samples within each specific emission standard, industrial stage, and types of raw materials, products, and fuels. Second, the integrated source profiles were synthesized by weighting these sub-category profiles according to their corresponding total VOC emissions. This method aligns with the national technical guidelines for integrated air pollutant emission inventories (Ministry of Ecology and Environment, 2024)."

Comment: *2. Section 3.1: The authors attribute the overestimation of ethanol in EP2 to the model's omission of temporary emission restrictions during and before the 2019 China International Import Expo (CIIE). To better evaluate the impact of these restrictions, could you provide model results excluding the CIIE period (e.g., by removing those days from the evaluation dataset)? This would help clarify how much of the bias is directly linked to unaccounted emission reductions and improve confidence in attributing the overestimation to this specific event.*

Response: Thank you for the insightful comment. After excluding data from the CIIE period, the observed concentrations of traditional VOCs and OVOCs, such as acetone (ACET), acrolein (ACRO), methyl ethyl ketone (MEK), and ethanol (ETOH), increased. The model performance for most species has been improved, particularly for alkenes, aromatic hydrocarbons, and most OVOCs (Table R1). For ETOH, the normalized mean bias (NMB) and normalized mean error (NME) decrease from 1.67 to -0.084 and from 2.45 to 0.80, respectively. As the temporary emission restrictions applied to major cities in the surrounding area of Shanghai and on the pollution transport pathway in Anhui and Jiangsu Provinces, all data during the CIIE period have been excluded from analysis to reduce potential influences from the temporary emission restrictions.

Table R1. Comparison of observed average concentrations of OVOCs and their VOC precursors (ppb), normalized mean bias (NMB), and normalized mean error (NME) during EP2 at the Shanghai monitoring site. Values outside and inside parentheses represent results with the CIIE period excluded and included, respectively.

Species	Obs	NMB	NME	Species	Obs	NMB	NME
HCHO	2.58 (2.75)	-0.21 (-0.29)	0.32 (0.36)	**OLE1**	0.14 (0.14)	3.31 (3.70)	3.31 (3.70)
CCHO	0.56 (0.60)	0.64 (0.48)	0.74 (0.63)	**OLE2**	0.28 (0.27)	1.71 (2.16)	1.77 (2.24)
ACRO	0.053 (0.048)	1.75 (1.81)	1.81 (1.87)	**BDE13**	0.011 (0.011)	8.8 (10.5)	8.8 (10.5)
ACET	1.89 (1.63)	-0.19 (-0.031)	0.43 (0.51)	**ACYE**	1.35 (1.38)	-0.25 (-0.21)	0.54 (0.53)
MACR	0.018 (0.021)	0.79 (0.33)	1.06 (0.82)	**ALK1**	6.83 (6.70)	-0.7 (-0.68)	0.7 (0.68)
MEK	0.64 (0.54)	0.17 (0.41)	0.59 (0.66)	**ALK2**	4.22 (4.17)	-0.63 (-0.63)	0.65 (0.64)
MVK	0.026 (0.034)	1.03 (0.64)	1.17 (1.00)	**ALK3**	2.62 (2.60)	-0.27 (-0.22)	0.47 (0.51)
RCHO	0.36	0.11	0.35	**ALK4**	2.42	0.48	0.69

	(0.44)	(-0.072)	(0.35)		(2.30)	(0.70)	(0.89)
ETOH	3.24 (1.33)	-0.084 (1.67)	0.80 (2.45)	**ALK5**	1.34 (0.98)	0.26 (0.98)	0.62 (1.21)
HCOOH	1.95 (3.57)	-0.96 (-0.98)	0.99 (0.98)	**ARO1**	0.45 (0.41)	1.3 (1.63)	1.4 (1.67)
CCOOH	2.59 (2.66)	-0.75 (-0.78)	0.76 (0.79)	**ARO2MN**	0.32 (0.27)	1.45 (2.02)	1.54 (2.07)
CRES	0.41 (0.50)	-0.51 (-0.67)	0.72 (0.78)	**BENZ**	0.47 (0.45)	0.73 (0.87)	0.8 (0.97)
PAN	0.61 (0.63)	-0.35 (-0.42)	0.40 (0.5)	**TOLU**	1.11 (1.05)	0.16 (0.19)	0.55 (0.72)
ETHE	1.96 (1.75)	0.16 (0.39)	0.55 (0.82)	**MPXYL**	0.63 (0.53)	1.48 (2.21)	1.58 (2.29)
PROP	0.58 (0.44)	1.39 (1.82)	1.57 (1.93)	**OXYL**	0.25 (0.22)	1.29 (1.90)	1.41 (2.00)
ISOP	0.019 (0.020)	0.23 (0.31)	0.79 (0.96)	**B124**	0.053 (0.046)	1.77 (2.39)	1.80 (2.41)

Comment: *3. Figure S7: Observational data indicate that ethanol concentrations were markedly lower during the CIIE period. Given that approximately 30−70% of total OVOCs originated from primary emissions, did other OVOC species such as HCHO show a similar decreasing trend during the same period?*

Response: Thank you for this valuable comment. We compared the concentrations of key OVOC species and traditional VOCs (i.e., alkanes, alkenes, and aromatic hydrocarbons) during the EP2 (Table R1). Most alkanes, alkenes, and aromatic hydrocarbons increased after excluding data from the CIIE period. Among OVOC species, ACET, ACRO, MEK, and ETOH increased, while HCHO, HCOOH, MVK, and RCHO decreased. The distinct responses among OVOCs may be attributed to differences in the relative contributions of their direct emissions and secondary formation from precursor oxidation production. In addition, variations in source-specific control strategies may lead to diverse changes in OVOC concentrations. To minimize potential impacts of temporary emission restrictions, both observed and modeled data during the CIIE period were excluded from the analysis in the revised manuscript.

Comment: *4. Line 171: In the manuscript, the authors state a temperature difference as "2.5 ℃ (16.8%) higher". Expressing a temperature change as a percentage can be misleading because the result depends on the choice of reference temperature and*

temperature scale (°C vs. K). For example, the same ΔT corresponds to ~16.8% if referenced to 14.9 °C, but only ~0.87% if referenced to the absolute temperature in Kelvin.

Response: Thank you for pointing this out. We agree with the reviewer that relative temperature changes can differ substantially depending on whether they are calculated using Celsius and Kelvin, which may introduce biases in the interpretation of temperature sensitivities.

Following suggestions from other reviewers, we have conducted additional sensitivity simulations by applying temperature-dependent adjustments to solvent use and gasoline evaporative OVOC emissions, following the approach used in our previous study (Qin et al. 2025). Compared with the original results, a general decreasing trend was found, particularly in the colder episode (EP2) (Fig. R1). This is because the daily maximum surface temperature during both episodes in regions strongly influenced by anthropogenic emissions remained below the reference temperature (25 °C) used to scale evaporative emissions based on temperature-dependent emission factors. We acknowledge that this adjustment approach is still subject to uncertainties, including the choice of reference temperature and potential variability in temperature dependence among different volatile species due to differences in vapor pressure. A more robust assessment of temperature-dependent evaporative emissions would require species-specific temperature-emission relationships from different sources, which is beyond the scope of the present study. To avoid confusion and potential misinterpretation, we have therefore removed the related discussion on the impacts of temperature-dependent evaporative emissions on OVOC simulations from the revised manuscript.

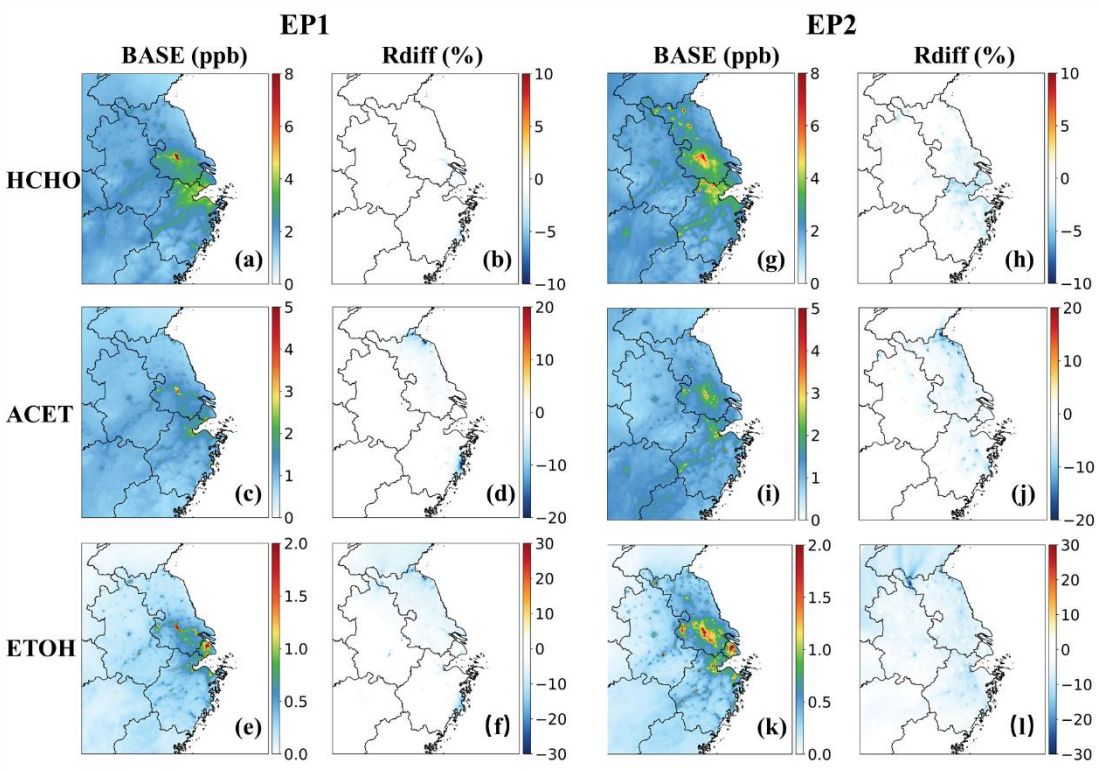

Figure R1. Episode averaged concentrations of HCHO, ACET, and ETOH in the base case (unit: ppb) and the relative changes due to temperature-adjusted evaporative emissions (Rdiff, (tempadj-base)/base %).

Comment: *5. Lines 213-214: The authors state that "Most OVOCs exhibited higher concentrations in EP2 than in EP1, except for MEOH", but this is not entirely consistent with the observational results, at least based on the comparison between Figs 2 and S6. Considering the short-term emission reductions during the CIIE period, the substantial decrease in anthropogenic OVOC emissions during EP2 should lead to reduced concentrations for some OVOCs.*

Response: Thank you for pointing this out. The different seasonal trends between modeled and observed OVOCs may likely be attributed to several reasons. Firstly, the temporary emission control during CIIE was not considered in model simulations, resulting in higher predicted OVOC concentrations during EP2. To assess this impact, data from the CIIE period were excluded. Although the observed concentrations of several OVOC species increased, most OVOCs, such as carbonyl species, remained higher during EP1 than in EP2 (Table S5), contrary to model predictions. This suggests that the discrepancy between modeled and observed seasonal OVOC trends is likely due to model biases. As shown in Table S5, most OVOCs are underestimated, with the biases being particularly pronounced during EP1. However, OVOC trends in other parts of the YRD may differ from those in Shanghai, due to the complexity of industrial processes in this region, a primary emission source of OVOCs and their precursors. Additional long-term observations at other sites would be helpful for a better

understanding of the seasonal variability of OVOCs in the YRD. To improve the clarity of the manuscript, the text has been revised as follows:
Lines 256-258: "In contrast to observations in Shanghai, the model predicted higher concentrations of most OVOCs in EP2 than in EP1 across the YRD, likely due to biases in the model representation of OVOCs (Table S5)."

A discussion on the modeled OVOC seasonal trends has been added in Section 4 as follows:
Lines 453-454: "The underestimation of OVOCs may result in biased predictions of their seasonal variability."

Comment: *6. Line 341: "facilitate" should be "facilitates".*
Response: The word has been revised.

Comment: *7. The authors mention that "In the HO2 pool, approximately 16.6% was newly generated, with OVOC photolysis being the dominant source (94.1%)". However, the presentation in Fig. 2c is somewhat misleading. It is recommended that the authors further clarify the relative proportions of "newly generated" HO2 and "primary" HO2 in Figure 2.*
Response: Thank you for this valuable comment. As HO_2, RO_2, and OH radicals are closely coupled and mutually interdependent, we now focus on primary radical production from photolysis of OVOCs, O_3, HONO, and ozonolysis of OVOCs and unsaturated VOCs, in which radicals are generated solely as products. Contributions from radical interconversion and cycling are therefore not included. Primary radicals initiate atmospheric radical chemistry and trigger radical chain reactions, ultimately leading to ozone accumulation. By focusing on the contribution of OVOCs to primary radical production, we provide a clearer and more robust assessment of their role in ozone formation. Overall, OVOC photooxidation is the dominant source of primary HO_2 across the YRD, accounting for more than 90% (Fig. 4). The figures and manuscript have been updated accordingly.

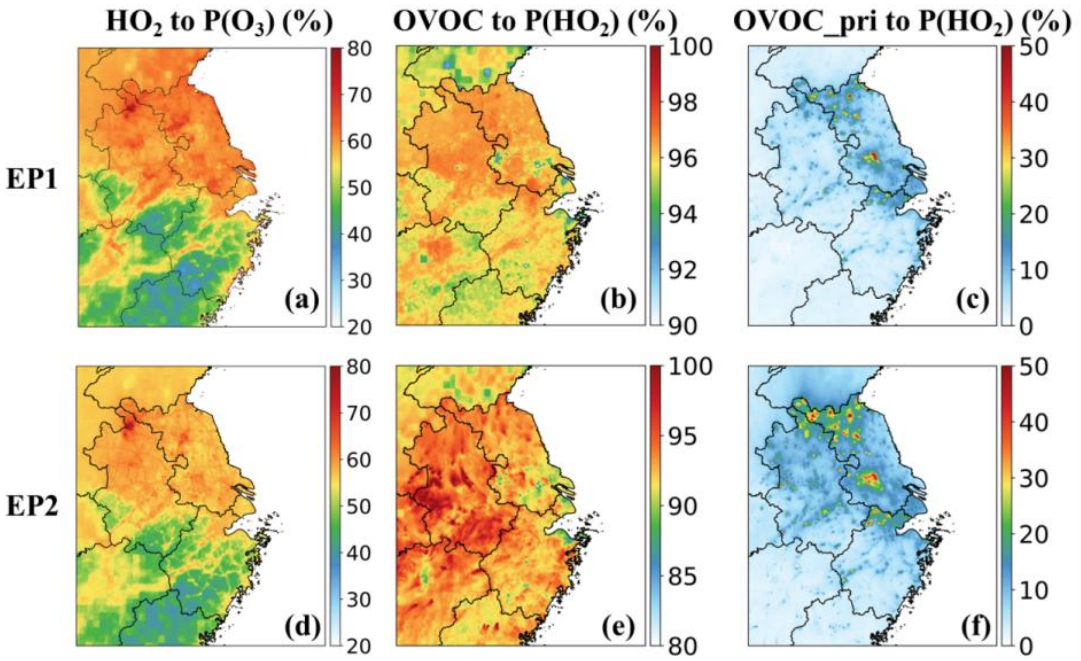

Figure 4. Daytime-averaged contributions of the HO_2 + NO pathway to ozone production rates (a, d), OVOC contributions to primary HO_2 radical production (b, e), and contributions from primary OVOCs (c, f) during the two episodes.

Reference

Qin, M. M., She, Y. L., Wang, M., Wang, H. L., Chang, Y. H., Tan, Z. F., An, J. Y., Huang, J., Yuan, Z. B., Lu, J., Wang, Q., Liu, C., Liu, Z. X., Xie, X. D., Li, J. Y., Liao, H., Pye, H. O. T., Huang, C., Guo, S., Hu, M., Zhang, Y. H., Jacob, D. J., and Hu, J. L.: Increased urban ozone in heatwaves due to temperature-induced emissions of anthropogenic volatile organic compounds, Nat. Geosci, 15, 10.1038/s41561-024-01608-w, 2025.